

Method for Detecting Berry's Phase in a Modified Paul Trap

Jong-Chan Park, Jeong-Young Ji,^{*} and Kwang-Sup Soh[†]

Department of Physics Education, Seoul National University, Seoul 151-742, Korea

Abstract

We modify the time-dependent electric potential of the Paul trap from a sinusoidal waveform to a square waveform. The exact quantum motion and the Berry's phase of an electron in the modified Paul trap are found in an analytically closed form. We consider a scheme to detect the Berry's phase by a Bohm-Aharonov-type interference experiment and point out a critical property which renders it practicable.

03.65.Bz

Typeset using REV_TE_X

^{*}Electronic address: jyji@phyb.snu.ac.kr

[†]Electronic address: kssoh@phyb.snu.ac.kr

I. INTRODUCTION

The Paul trap is an instrument which suspends free charged and neutral particles without material walls. Such traps permit the observation of isolated particles, even a single one, over a long period of time [1]. The Hamiltonian of the Paul trap has the form of a time-dependent harmonic oscillator,

$$H(t) = \frac{1}{2m}p^2(t) + \frac{1}{2}m\omega^2(t)q^2(t) \quad (1.1)$$

whose effective spring constant is of the form [2]

$$k(t) = a + b \cos(2\pi t/\tau). \quad (1.2)$$

The quantum motion of the Paul trap has been studied in Refs. [2–4]. It is well known that the generalized invariant for Eq. (1.1) can be written as [5]

$$I(t) = g_-(t)\frac{p^2}{2} + g_0(t)\frac{pq + qp}{2} + g_+(t)\frac{q^2}{2}. \quad (1.3)$$

Here, using the classical solutions satisfying

$$\ddot{f}_{1,2}(t) + \omega^2(t)f_{1,2}(t) = 0, \quad (1.4)$$

we have [4]

$$\begin{aligned} g_-(t) &= c_1 f_1^2(t) + c_2 f_1(t)f_2(t) + c_3 f_2^2(t), \\ g_0(t) &= -m\{c_1 f_1(t)\dot{f}_1(t) \\ &\quad + (c_2/2)[\dot{f}_1(t)f_2(t) + f_1(t)\dot{f}_2(t)] \\ &\quad + c_3 f_2(t)\dot{f}_2(t)\}, \\ g_+(t) &= m^2[c_1 \dot{f}_1^2(t) + c_2 \dot{f}_1(t)\dot{f}_2(t) + c_3 \dot{f}_2^2(t)] \end{aligned} \quad (1.5)$$

where c_1 , c_2 , and c_3 are arbitrary constants.

Recently, Ji et al. [6] found the exact eigenfunctions of $I(t)$:

$$\begin{aligned} \psi_n(q, t) = & \frac{1}{\sqrt{2^n n!}} \left(\frac{\omega_I}{\pi g_-(t)} \right)^{\frac{1}{4}} e^{-i \frac{g_0(t)}{2g_-(t)} q^2} \\ & \times e^{-i \int dt \frac{\omega_I}{mg_-(t)} (n + \frac{1}{2})} e^{-\frac{\omega_I}{2g_-(t)} q^2} H_n \left(\sqrt{\frac{\omega_I}{g_-(t)}} q \right) \end{aligned} \quad (1.6)$$

where H_n is Hermite polynomial. For a time-periodic quantum harmonic oscillator, analyzing the wave function in Eq. (1.6), they constructed a cyclic initial state (CIS) such that $\psi_n(t + \tau') = e^{i\chi_n(\tau')} \psi_n(t)$ with

$$\chi_n(\tau') = - \left(n + \frac{1}{2} \right) \int_0^{\tau'} \frac{\omega_I}{mg_-(t)} dt. \quad (1.7)$$

and calculated the corresponding Berry's phase (see Ref. [7] for the Berry's phase and Ref. [8] for its nonadiabatic generalization). Subsequently, a new type of CIS, whose period is a multiple of the period of the Hamiltonian, was found [9].

In this paper, we modify the time-periodic electric potential from the sinusoidal waveform in Eq. (1.2) to a square waveform. This square potential has stable classical solutions, as the sinusoidal potential does. This means that we can suspend charged particles using this modified potential, as we do in the original Paul trap. Furthermore, the classical solutions of this modified Paul trap are very simple, so we can calculate the exact quantum solutions in a simple closed form. (Note that the classical solutions of the original Paul trap are Mathieu functions, which are difficult to deal with.) The purpose of this paper is to find the Berry's phase for the modified Paul trap and to propose an experimental scheme to detect it.

As seen from Eq. (1.5), there is an arbitrariness in fixing the invariant, and hence the complete set of the Fock space (eigenstates of the invariant). Therefore, we should show that the phase change of an eigenstate, Eq. (1.6), is irrelevant to which invariant we choose. There is another problem: When we let the electron beam pass through the modified Paul trap, it seems that we should have a single eigenstate for a coherent interference pattern. However, it turns out that if we prepare a plane wave of the electron – which can be expanded as the eigenstates in Eq. (1.6) – we get a coherent interference pattern.

In Sec. II, we apply the result of Refs. [4], [6], and [9] to the modified Paul trap to find the exact quantum state and the Berry's phase. In Sec. III, we present a Bohm-Aharonov-type

experimental method for detecting the Berry's phase of this system. The key feature which renders this experiment practicable is that the phase change is independent of the invariant we choose, and for a coherent interference pattern it is sufficient to prepare a plane wave entering the trap. A summary and discussions are given in the last section.

II. EXACT QUANTUM MOTION OF THE MODIFIED PAUL TRAP

A. Quantum Mechanics of the Paul Trap

The classical and quantum motion of an electron in the Paul trap is described by the following Hamiltonian [1]:

$$H(t) = H_x(t) + H_y(t) + H_z(t) \quad (2.1)$$

where

$$H_x = \frac{1}{2m}p_x^2 + \frac{1}{2}m\omega_x^2x^2, \quad (2.2a)$$

$$H_y = \frac{1}{2m}p_y^2 + \frac{1}{2}m\omega_y^2y^2, \quad (2.2b)$$

$$H_z = \frac{1}{2m}p_z^2. \quad (2.2c)$$

Here, the Hamiltonians of the x - and the y -motions have the form of a time-dependent harmonic oscillator with

$$\omega_x^2 = \frac{e\Phi(t)}{md^2} = -\omega_y^2 \quad (2.3)$$

where

$$\Phi(t) = U + V \cos(2\pi t/\tau). \quad (2.4)$$

is an applied voltage, d is the gap of the walls of the Paul trap, and e is the absolute value of the electron charge.

The wave function of this system satisfies the time-dependent Schrödinger equation

$$i\frac{\partial}{\partial t}\Psi(x, y, z, t) = H(t)\Psi(x, y, z, t). \quad (2.5)$$

Using the method of separation of variables, we have three independent equations:

$$i\frac{\partial}{\partial t}\Psi_i(\mathbf{r}_i, t) = H_i(t)\Psi_i(\mathbf{r}_i, t), \quad (i = x, y, z). \quad (2.6)$$

Here, the equation in the z -direction gives the plane-wave solution $\Psi_z(z, t) = e^{i(k_z z - E_z t)}$. In addition, since Eqs. (2.2a) and (2.2b) are the Hamiltonian of a time-dependent harmonic oscillator, we can find Ψ_x and Ψ_y using the methods found in Refs. [4] and [6].

B. Modified Paul Trap

Now, we modify the applied voltage from the form in Eq. (2.4) to the following square wave form (see Fig. 1):

$$\Phi(t) = \begin{cases} \Phi_1 > 0, & \text{for } \tau_2 - \tau < t - r\tau < -\tau_2, \\ \Phi_2 < 0, & \text{for } -\tau_2 < t - r\tau < \tau_2, \end{cases} \quad (2.7)$$

where r is an integer. Then, the frequencies of H_x and H_y are described by

$$\omega_x^2(t) = \begin{cases} \omega_1^2, & \text{for } \tau_2 - \tau < t - r\tau < -\tau_2, \\ -\omega_2^2, & \text{for } -\tau_2 < t - r\tau < \tau_2, \end{cases} \quad (2.8a)$$

$$\omega_y^2(t) = \begin{cases} -\omega_1^2, & \text{for } \tau_2 - \tau < t - r\tau < -\tau_2, \\ \omega_2^2, & \text{for } -\tau_2 < t - r\tau < \tau_2, \end{cases} \quad (2.8b)$$

where

$$\omega_1^2 = \frac{e|\Phi_1|}{2md^2}, \quad \omega_2^2 = \frac{e|\Phi_2|}{2md^2}. \quad (2.9)$$

FIGURES

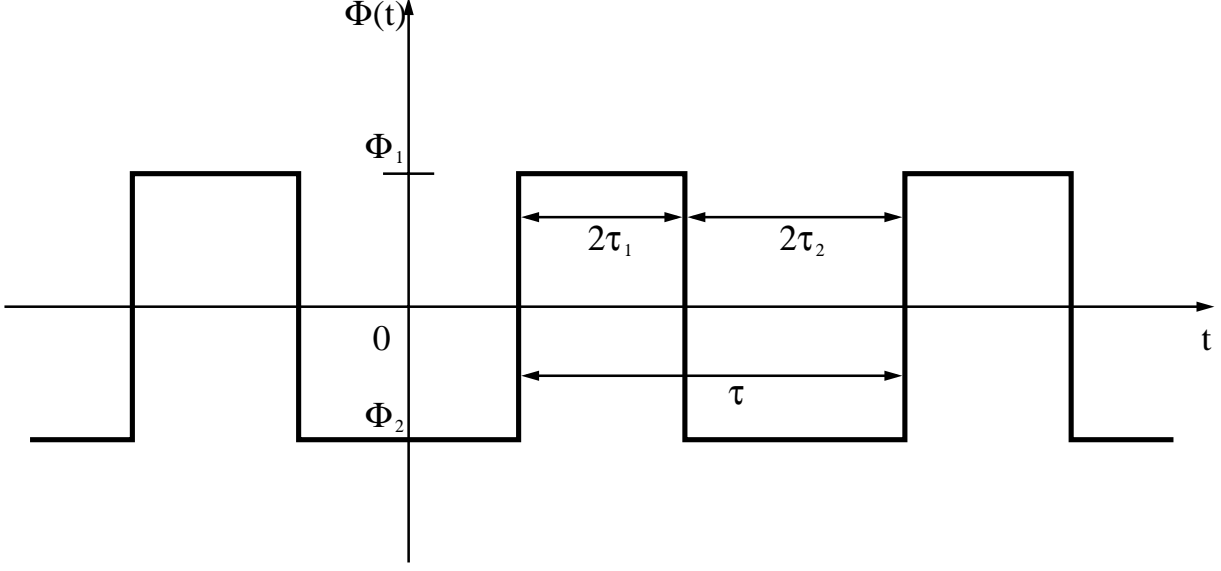


FIG. 1. The time-dependent potential of a square waveform.

In order to study the quantum mechanics of this system, it is necessary to determine independent classical solutions of Eq. (1.4) for the x - and the y -components with Eqs. (2.8a) and (2.8b), respectively. These solutions are fully analyzed in Ref. [9]. Since the effective spring constant of the modified Paul trap alternates between positive and *negative* values, we should check carefully that the solutions of Ref. [9] are applicable in this model. After tedious calculations, we verified that our classical solutions are identical with the solutions of Ref. [9] with the replacements of ω_2 by $-i\omega_2$ in the x -component and ω_1 by $-i\omega_1$ in the y -component.

As a result, we find the classical solutions for the x -component to be

$$f_x(t) = \begin{cases} A_{x,r}e^{i\omega_1(t-r\tau)} + B_{x,r}e^{-i\omega_1(t-r\tau)}, & \text{for } \tau_2 - \tau < t - r\tau < -\tau_2, \\ C_{x,r}e^{\omega_2(t-r\tau)} + D_{x,r}e^{-\omega_2(t-r\tau)}, & \text{for } -\tau_2 < t - r\tau < \tau_2, \end{cases} \quad (2.10)$$

where

$$\begin{pmatrix} C_{x,r} \\ D_{x,r} \end{pmatrix} = \frac{1}{2} \begin{pmatrix} (1 + i\omega_1/\omega_2)e^{-i\omega_1\tau_2 + \omega_2\tau_2} & (1 - i\omega_1/\omega_2)e^{i\omega_1\tau_2 + \omega_2\tau_2} \\ (1 - i\omega_1/\omega_2)e^{-i\omega_1\tau_2 - \omega_2\tau_2} & (1 + i\omega_1/\omega_2)e^{i\omega_1\tau_2 - \omega_2\tau_2} \end{pmatrix} \begin{pmatrix} A_{x,r} \\ B_{x,r} \end{pmatrix}. \quad (2.11)$$

The coefficients $A_{x,r}$ and $B_{x,r}$, belonging to successive values of r , can be related by a matrix

P obtained by imposing continuity for $f_x(t)$ and its derivative at $t = -\tau_2 + r\tau$ and $t = \tau_2 + r\tau$.

These lead to

$$\begin{pmatrix} A_{x,r} \\ B_{x,r} \end{pmatrix} = P^r \begin{pmatrix} A_{x,0} \\ B_{x,0} \end{pmatrix}, \quad (2.12)$$

with

$$P = \begin{pmatrix} (\alpha_{x,1} - i\beta_{x,1})e^{i\omega_1\tau} & -i\beta_{x,2}e^{i\omega_1\tau} \\ i\beta_{x,2}e^{-i\omega_1\tau} & (\alpha_{x,1} + i\beta_{x,1})e^{-i\omega_1\tau} \end{pmatrix}, \quad (2.13)$$

where

$$\alpha_{x,1} = \cos 2\omega_1\tau_2 \cosh 2\omega_2\tau_2 + \frac{\eta}{2} \sin 2\omega_1\tau_2 \sinh 2\omega_2\tau_2, \quad (2.14a)$$

$$\beta_{x,1} = \sin 2\omega_1\tau_2 \cosh 2\omega_2\tau_2 - \frac{\eta}{2} \cos 2\omega_1\tau_2 \sinh 2\omega_2\tau_2, \quad (2.14b)$$

$$\beta_{x,2} = \frac{\epsilon}{2} \sinh 2\omega_2\tau_2, \quad (2.14c)$$

and

$$\epsilon = \frac{\omega_1}{\omega_2} + \frac{\omega_2}{\omega_1}, \quad \eta = \frac{\omega_1}{\omega_2} - \frac{\omega_2}{\omega_1}, \quad (2.15)$$

where $\alpha_{x,1}$, $\beta_{x,1}$, and $\beta_{x,2}$ satisfy the condition

$$\alpha_{x,1}^2 + \beta_{x,1}^2 - \beta_{x,2}^2 = 1. \quad (2.16)$$

Solving the eigenvalue problem for the matrix P , we find the eigenvalues

$$p_{\pm} = \lambda_x \pm \sqrt{\lambda_x^2 - 1} \quad (2.17)$$

where $\lambda_x = \alpha_{x,1} \cos \omega_1\tau + \beta_{x,1} \sin \omega_1\tau$, and their corresponding eigenvectors

$$\begin{pmatrix} A_{x,0} \\ B_{x,0} \end{pmatrix} \propto \begin{pmatrix} \beta_{x,2}e^{i\omega_1\tau} \\ \nu_x \pm i\sqrt{\lambda_x^2 - 1} \end{pmatrix} \quad (2.18)$$

where $\nu_x = \alpha_{x,1} \sin \omega_1\tau - \beta_{x,1} \cos \omega_1\tau$. If $|\lambda_x| \leq 1$, p_{\pm} are complex conjugates. Investigating the form of the matrix P , it is easy to find that the solutions corresponding to two eigenvalues

are also complex conjugates. Therefore, the two independent solutions are taken to be the real and the imaginary parts of one of them. In this case, we can set

$$A_{x,0} = \beta_{x,2}e^{i\omega_1\tau}, \quad B_{x,0} = \nu_x - \sqrt{1 - \lambda_x^2} \quad (2.19)$$

with one eigenvalue

$$p_+ = \lambda_x + i\sqrt{1 - \lambda_x^2} = e^{i\phi_x} \quad (2.20)$$

where $\tan \phi_x = \sqrt{1 - \lambda_x^2}/\lambda_x$. Then, the classical solution for $|\lambda_x| \leq 1$ can be written as

$$f_x(t) = \begin{cases} e^{ir\phi_x} [A_{x,0}e^{i\omega_1(t-r\tau)} + B_{x,0}e^{-i\omega_1(t-r\tau)}], & \text{for } \tau_2 - \tau < t - r\tau < -\tau_2, \\ e^{ir\phi_x} [C_{x,0}e^{\omega_2(t-r\tau)} + D_{x,0}e^{-\omega_2(t-r\tau)}], & \text{for } -\tau_2 < t - r\tau < \tau_2. \end{cases} \quad (2.21)$$

In the same way, we have the classical solution for the y -component:

$$f_y(t) = \begin{cases} e^{ir\phi_y} [A_{y,0}e^{\omega_1(t-r\tau)} + B_{y,0}e^{-\omega_1(t-r\tau)}], & \text{for } \tau_2 - \tau < t - r\tau < -\tau_2, \\ e^{ir\phi_y} [C_{y,0}e^{i\omega_2(t-r\tau)} + D_{y,0}e^{-i\omega_2(t-r\tau)}], & \text{for } -\tau_2 < t - r\tau < \tau_2, \end{cases} \quad (2.22)$$

with

$$A_{y,0} = \beta_{y,2}e^{\omega_1\tau}, \quad B_{y,0} = \nu_y - i\sqrt{1 - \lambda_y^2}, \quad (2.23)$$

$$\begin{pmatrix} C_{y,0} \\ D_{y,0} \end{pmatrix} = \frac{1}{2} \begin{pmatrix} (1 - i\omega_1/\omega_2)e^{-\omega_1\tau_2 + i\omega_2\tau_2} & (1 + i\omega_1/\omega_2)e^{\omega_1\tau_2 + i\omega_2\tau_2} \\ (1 + i\omega_1/\omega_2)e^{-\omega_1\tau_2 - i\omega_2\tau_2} & (1 - i\omega_1/\omega_2)e^{\omega_1\tau_2 - i\omega_2\tau_2} \end{pmatrix} \begin{pmatrix} A_{y,0} \\ B_{y,0} \end{pmatrix}, \quad (2.24)$$

where

$$\nu_y = \alpha_{y,1} \sinh \omega_1\tau - \beta_{y,1} \cosh \omega_1\tau, \quad (2.25)$$

$$\alpha_{y,1} = \cosh 2\omega_1\tau_2 \cos 2\omega_2\tau_2 - \frac{\eta}{2} \sinh 2\omega_1\tau_2 \sin 2\omega_2\tau_2, \quad (2.26a)$$

$$\beta_{y,1} = \sinh 2\omega_1\tau_2 \cos 2\omega_2\tau_2 - \frac{\eta}{2} \cosh 2\omega_1\tau_2 \sin 2\omega_2\tau_2, \quad (2.26b)$$

$$\beta_{y,2} = \frac{\epsilon}{2} \sin 2\omega_2\tau_2, \quad (2.26c)$$

and

$$e^{i\phi_y} = \lambda_y + i\sqrt{1 - \lambda_y^2} \quad (2.27)$$

where $\lambda_y = \alpha_{y,1} \cosh \omega_1 \tau - \beta_{y,1} \sinh \omega_1 \tau$.

The two independent real solutions $f_1(t)$ and $f_2(t)$ are given by

$$f_1(t) = \frac{1}{2}[f(t) + f^*(t)], \quad f_2(t) = \frac{1}{2i}[f(t) - f^*(t)] \quad (2.28)$$

for the x and the y components, respectively. These solutions exhibit stable motions for $\lambda \leq 1$ (λ stands for λ_x or λ_u); that is, they oscillate with bounded amplitudes.

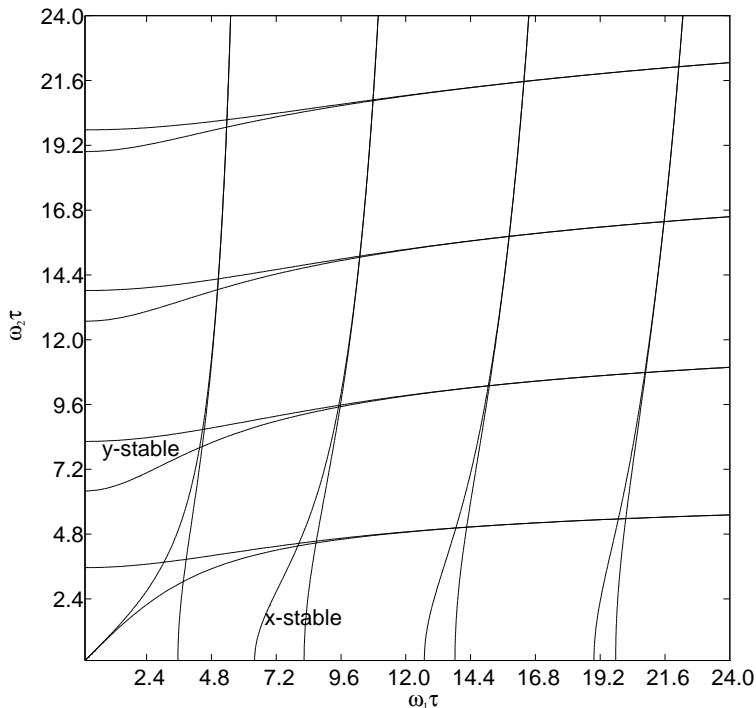


FIG. 2. The stability-instability diagram. The vertical strips stand for the stable regions in the x -motion, the horizontal strips for the y -motion.

It is important to know the stable regions in ω_1 - ω_2 diagram where the classical solutions are stable. For $\tau_1 = \tau_2$, we present the stable regions and the unstable regions in Fig. 2. This map is similar to the stability diagram obtained from the Mathieu equation. Only the overlapping regions of the x -stable and the y -stable regions are of our interest. Therein, the motion is stable both in the x -direction and the y -direction. On the other hand, when $|\lambda| > 1$, the solutions diverge at $t \rightarrow \infty$ or $t \rightarrow -\infty$ as discussed in Ref. [9].

Now, we fix the generalized invariant by fixing c_1 , c_2 , and c_3 in Eq. (1.5). For example, to find $I(t)$ such that $I(t) = H(t_0)$ in the x -component (t_0 denotes the initial time), we fix those three parameters as [10]

$$\begin{aligned}
c_{x,1} &= \frac{\beta_{x,2}^2 + B_{x,0}^2 - 2\beta_{x,2}B_{x,0} \cos \omega_1 \tau}{m(\beta_{x,2}^2 - B_{x,0}^2)^2}, \\
c_{x,2} &= \frac{-4\beta_{x,2}B_{x,0} \sin \omega_1 \tau}{m(\beta_{x,2}^2 - B_{x,0}^2)^2}, \\
c_{x,3} &= \frac{\beta_{x,2}^2 + B_{x,0}^2 + 2\beta_{x,2}B_{x,0} \cos \omega_1 \tau}{m(\beta_{x,2}^2 - B_{x,0}^2)^2}.
\end{aligned} \tag{2.29}$$

In this way, we can get the exact wave function of the modified Paul trap, Eq. (1.6), and the phase change (which includes the Berry's phase) for a period, Eq. (1.7).

III. EXPERIMENTAL METHOD OF DETECTING BERRY'S PHASE

A. $N\tau$ -periodic Wave Function

In this section, we present an experimental method to detect the effect of the Berry's phase. The existence of the CIS is provided by the periodic classical solutions. As discussed in Refs. [6] and [9], if it holds in Eqs. (2.21) and (2.22) that

$$\phi = \frac{l}{N'} 2\pi \quad (l, N' = \text{integers and } N' \neq 0) \tag{3.1}$$

(where the index of x and y is understood), the classical solution is $N'\tau$ -periodic. Then, $g_-(t)$ is $N'\tau/\epsilon$ -periodic ($\epsilon = 1$ for odd N' , $\epsilon = 2$ for even N'), accordingly, so is the wave function in Eq. (1.6).

When we have two independent real classical solutions, say $f_1(t)$ and $f_2(t)$, we can always construct the complex solution as

$$f_c(t) = d_1 f_1(t) + (d_2 + id_3) f_2(t), \tag{3.2}$$

where d_1 , d_2 , and d_3 ($d_1 d_3 \neq 0$) are real parameters. This solution can be written in polar form [11]:

$$f_c(t) = |f_c(t)|e^{i\theta(t)} \quad (3.3)$$

where

$$\theta(t) = \int_0^t \frac{\omega_I}{m|f_c(t')|^2} dt'. \quad (3.4)$$

If we set $c_1 = d_1^2$, $c_2 = 2d_1d_2$, and $c_3 = d_2^2 + d_3^2$, we have $g_-(t) = |f_c(t)|^2$. Then, the quantum phase, Eq. (1.7), of the n -th eigenstate, which is also a CIS with a period τ' , can be rewritten as

$$\chi_n(\tau') = -\left(n + \frac{1}{2}\right)\theta(\tau'). \quad (3.5)$$

Now we are ready to prove that the quantum phase in Eq. (3.5) is independent of the choice of the invariant. That is, the phase change of the eigenfunction of the invariant does not depend on what values of c_i we choose. The proof is as follows: If we assume that the phase change of the classical solution in Eq. (3.3) is altered by varying the parameter values $d_i (i = 1, 2, 3)$ or c_i , then there are many classical solutions corresponding to the respective periods. However, this contradicts the fact that the classical solution of Eq. (1.4) has only two independent solutions and that they are the real and the imaginary parts of Eq. (3.3). This completes our proof.

B. Experimental Setting

Now let us consider the experimental arrangement. Suppose we have a single coherent electron beam which is split into two parts, and suppose each part is allowed to enter the modified Paul trap, as shown in Fig. 3

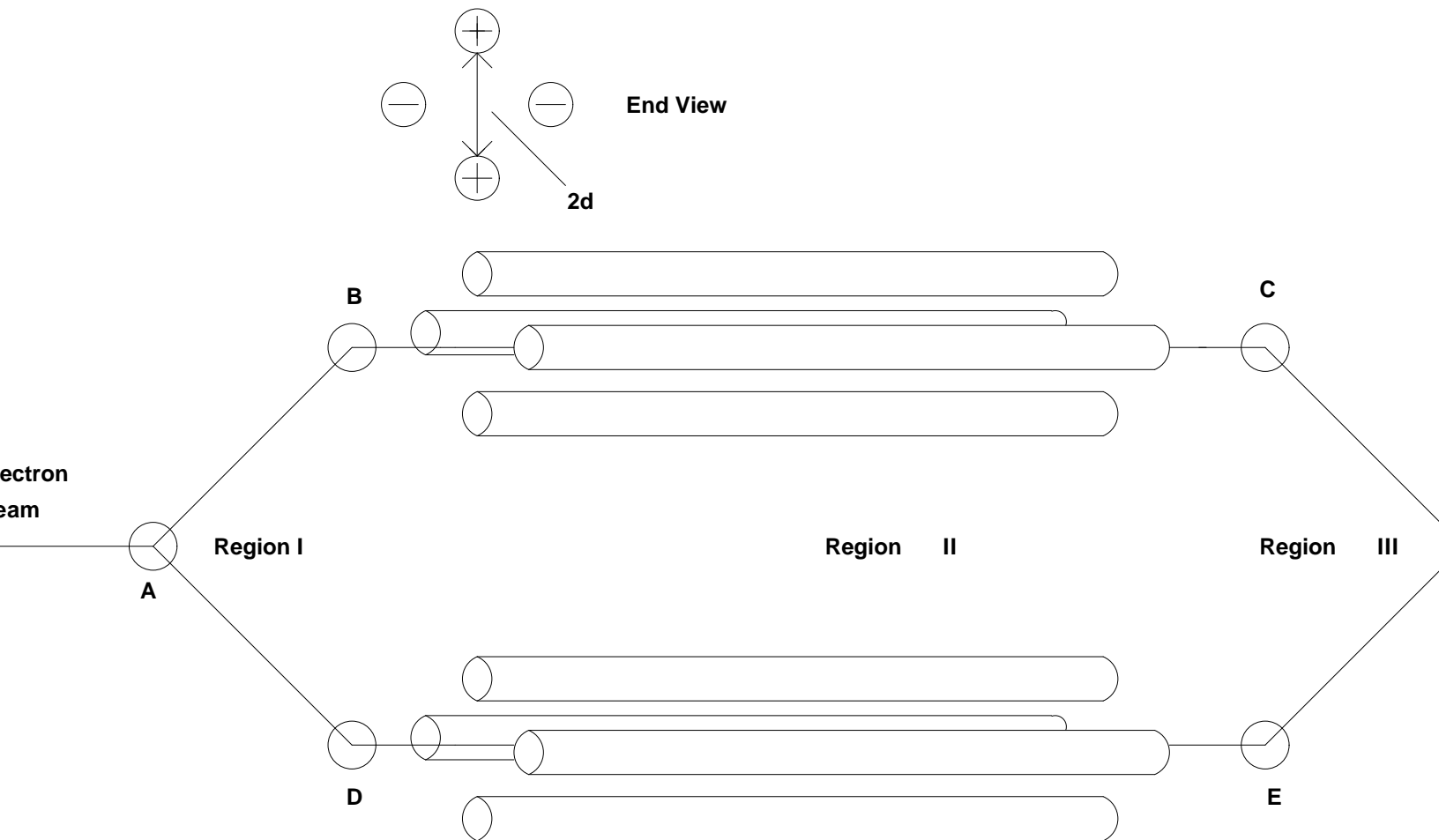


FIG. 3. The schematic diagram of the experimental arrangement.

This experiment is similar to the experiment illustrated by Aharonov and Bohm in Ref. [12]. After the beams pass through the modified Paul traps, they are combined to interfere coherently at the point F. Let us denote the paths A-B-C-F and A-D-E-F by path 1 and 2, respectively. The electric potential vanishes in region I so that the wave function of the electron is described by a plane wave which propagates along the z -direction: $\Psi(\text{I}) = L^{-3/2} e^{ik_z z - E_z t}$ where L is a suitable normalization factor. In region II, the potential varies as a function of time according to Eq. (2.7), $\Phi(t)$ and $-\Phi(t)$ in the x - and the y -directions, respectively, but Φ_1 and/or Φ_2 have different values for paths 1 and 2. When the electron is in region III, the potential vanishes again.

Let Ψ_1 and Ψ_2 be the wave functions that pass through path 1 and path 2, respectively. In region I, $\Psi(I) = \Psi_1(I) = \Psi_2(I)$. Then, as they enter region II, the two wave functions suffer different potentials in the two different Paul traps. Finally, we have $\Psi(\text{III}) = \Psi_1(\text{III}) + \Psi_2(\text{III})$ in region III.

In order to form a sharp interference pattern, it is necessary to have the wave functions at point F be of the form

$$\Psi(\text{III}) = \Psi(I)e^{-i\Theta_1} + \Psi(I)e^{-i\Theta_2}, \quad (3.6)$$

such that the pattern depends upon the phase difference $\Theta_2 - \Theta_1$. We emphasize that the critical factor which renders our experimental scheme practical is that any plane wave which splits at the point A does interfere at F, as required, in the form of Eq. (3.6).

Firstly, when Ψ_{1x} is a single eigenstate of the LR invariant, the phase change can be easily obtained by using Eq. (1.7), and it is evident the final wave function at F is of the form of Eq. (3.6). Next, for a plane wave propagating along the z -direction with the wave number \mathbf{k} ,

$$\mathbf{v} = \frac{\hbar\mathbf{k}}{m} = \frac{D}{T}\hat{z} \quad (3.7)$$

gives a final wave function of the form of Eq. (3.6), as we will see below. Here, D is the length of the Paul trap, and T is a multiple of the minimal period of the CIS, which can be controlled by the applied voltage. In this situation, the wave function of the electron entering the Paul trap is expanded in terms of eigenstates of the LR invariant [13]:

$$\Psi_{1x}(t) = \sum_{n=0,2,4,\dots} C_{1,n}\psi_{1,n}(x,t) \quad (3.8)$$

(Ψ_{1y} , Ψ_{2x} , and Ψ_{2y} can be expanded in a similar manner.) When the electrons leave the Paul trap, using Eq. (1.7) or (3.5), we have

$$\Psi_{1x}(t+T) = \sum_{n=0}^{\infty} C_{1,2n}\psi_{1,2n}(x,t)e^{-i(2n+\frac{1}{2})\theta_{1x}(T)}. \quad (3.9)$$

Further, in the phase of each eigenstate, the periodicity of the classical solution means that $2n\theta_{1x}(T)$ is a multiple of 2π . Therefore, we can write

$$\Psi_{1x}(t+T) = e^{-\frac{i}{2}\theta_{1x}(T)} \sum_{n=0}^{\infty} C_{1,2n} \psi_{1,2n}(x, t) \quad (3.10)$$

$$= e^{-\frac{i}{2}\theta_{1x}(T)} \Psi_{1x}(t). \quad (3.11)$$

In the same way, we have

$$\Psi_{1y}(t+T) = e^{-\frac{i}{2}\theta_{1y}(T)} \Psi_{1y}(t). \quad (3.12)$$

Then, we have the total wave function which travels path 1:

$$\Psi_1(t+T) = e^{-\frac{i}{2}[\theta_{1x}(T)+\theta_{1y}(T)]} e^{-i\theta_z} \Psi_1(t), \quad (3.13)$$

for path 2, we have

$$\Psi_2(t+T) = e^{-\frac{i}{2}[\theta_{2x}(T)+\theta_{2y}(T)]} e^{-i\theta_z} \Psi_2(t). \quad (3.14)$$

Therefore, the phase difference between two paths is

$$\Theta_2 - \Theta_1 = \frac{1}{2} \{ [\theta_{2x}(T) + \theta_{2y}(T)] - [\theta_{1x}(T) + \theta_{1y}(T)] \} \quad (3.15)$$

$$= \theta_2(T) - \theta_1(T). \quad (3.16)$$

Here, we have omitted the indices x and y since the phase changes for a period are equal in the x - and the y -directions.

C. Expected Results

In this section, we present a typical experimental scheme. In region III, we have the detector F, and we have a destructive interference when

$$|\theta_2 - \theta_1| = \pi. \quad (3.17)$$

This destructive interference of the two wave functions, via path 1 and 2, can be obtained by controlling the applied voltage or the velocity of the electron beams. By noting the fact that when Eq. (3.1) holds, the phase change over the minimal period is

$$\theta(\tau' = N'\tau/\epsilon) = l\pi, \quad (3.18)$$

we have two methods to obtain destructive interference. Firstly, we can control the applied voltages Φ_1 and Φ_2 so that $l = 1$ in Eq. (3.1) and $N'_1 = 2N'_2$ (where N'_1 and N'_2 are the values of N' for path 1 and path 2, respectively). Further, we can control the velocity of the electron beam so that

$$v = \frac{D}{N'_1\tau} \quad (T = N'_1\tau). \quad (3.19)$$

Then we have $\theta_1 = \pi$ and $\theta_2 = 2\pi$. Secondly, we can control the voltage values so that $l = 1$ and $l = 2$ with the same N' . From Eq. (3.18), it is clear that two wave functions interfere destructively. In Table 1, we present the numerical values of ω_1 and ω_2 for $N' = 4, 8$ with $l = 1$ and for $N' = 3$ with $l = 1, 2$.

TABLES

Table 1. Numerical values of ω_1 and ω_2 for $N\tau$ -periodic CISs ($N = 2, 3, 4$)

Fig. 4	l	N'	$\omega_1\tau = \omega_2\tau$	$\theta(\tau')$
a	1	4	3.14159	$\pi/2$
b	1	8	2.30517	$\pi/2$
c	1	3	2.63690	$\pi/2$
d	2	3	3.48328	π

The graphs of $g_-(t)$ in the x -direction for all the cases in Table 1 are shown in Fig. 4. The parameters are fixed as in Eq. (2.29), and hence the region of $g_-(t) = 1/m$ (the figures are depicted in $m = 1$ units) reflects that $I(t) = H(t)$, as discussed in Ref. [6]. By shifting these figures by a half period, $\tau/2$, we can also get $g_-(t)$ in the y -direction. As expected, they are $N\tau$ -periodic ($N = 2, 3, 4$), as are their corresponding wave functions, Eq. (1.6). The original and the shifted figures also reveal that the probability density function $|\Psi(x, y, t)|^2$ spreads in the x -direction and the y -direction alternately.

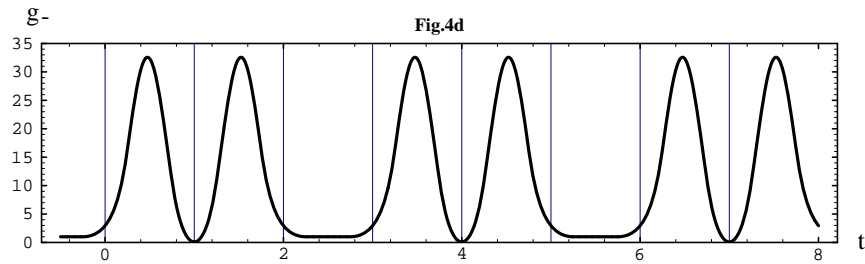
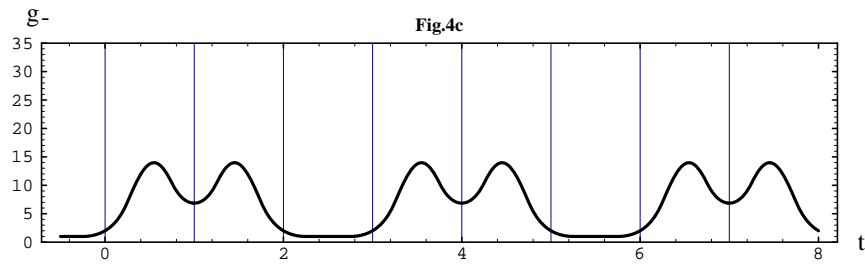
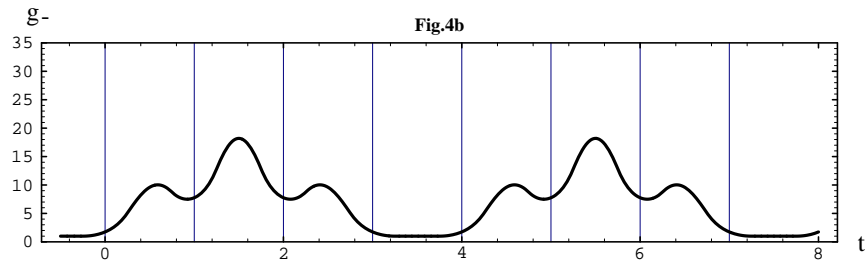
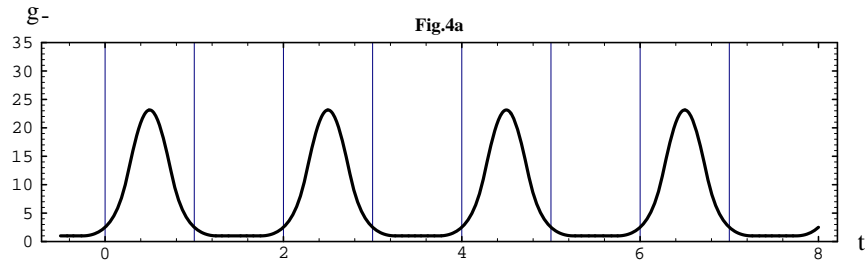


FIG. 4. The shapes of $g_-(t)$ for Table 1. The time is denoted in units of τ .

IV. DISCUSSION

Modification of the time-dependent electric potential of the Paul trap from a sinusoidal waveform to a square waveform gives a quantum solution with a simple mathematical form. Therefore, we can verify the existence of the $N\tau$ -periodic CIS and propose a method to detect the corresponding Berry's phase by experiment.

We estimate the values of the parameters for a practical experiment. To obtain an interference pattern successfully, we should have a Paul trap of submillimeter size ($d \sim 10^{-3}$ m). Considering a Paul trap whose length D is of the order of 10^{-1} m and an electron with a speed on the order of 10^6 m/s, $\tau' \sim 10^{-7}$ s, we have $\omega_1 \sim 10^8$ s $^{-1}$ from Table 1 and $\Phi \sim 1$ V from Eq. (2.9). For example, for $N' = 4$, $l = 1$ in Table 1, $D \approx 6$ cm, $d \approx 1$ mm, and $v \approx 5 \times 10^6$ m/s, we have $\tau \approx 6 \times 10^{-9}$ s, $\omega_{(1,2)} \approx 5 \times 10^8$ s $^{-1}$, and $|\Phi_{(1,2)}| \approx 1$ V. These values seem practical for an experimental arrangement.

There have been many applications and tests of the Berry's phase using an optical fiber [14], nuclear magnetic resonance (NMR) [15], etc. [16]. Nonetheless, there are no experiments about the Berry's phase caused by the quantum motions in phase space. (Note that the optical phase effect deals with the phenomena of classical electromagnetism, and the NMR experiment investigates the interaction between the spin and the external magnetic fields.) Our proposal will be a new experiment to detect the Berry's phase caused by a pure dynamics in phase space, and we expect that it will play a significant role in understanding the quantum motions of a time-dependent system in phase space.

V. ACKNOWLEDGMENTS

This work was supported by the Center for Theoretical Physics at Seoul National University and by the Basic Science Research Institute Program, Ministry of Education, Project No. BSRI-96-2418.

REFERENCES

- [1] W. Paul, Rev. Mod. Phys. **62**, 531 (1990).
- [2] L. S. Brown, Phys. Rev. Lett. **66**, 527 (1991).
- [3] M. Feng and K. Wang, Phys. Lett. A **197**, 135 (1995).
- [4] J. Y. Ji, J. K. Kim, and S. P. Kim, Phys. Rev. A **51**, 4268 (1995).
- [5] H. R. Lewis, Jr., and W. B. Riesenfeld, J. Math. Phys. **10**, 1458 (1969).
- [6] J. Y. Ji, J. K. Kim, S. P. Kim, and K. S. Soh, Phys. Rev. A **52**, 3352 (1995).
- [7] M. V. Berry, Proc. R. Soc. Lond. A **392**, 45 (1984).
- [8] Y. Aharonov and J. Anandan, Phys. Rev. Lett. **58**, 1593 (1987).
- [9] J. Y. Ji and J. K. Kim, Phys. Lett. A **208**, 25 (1995).
- [10] J. Y. Ji and J. K. Kim, Phys. Rev. A **53**, 703 (1996).
- [11] W. Magnus and S. Winkler, *Hill's Equation* (Dover, New York, 1966).
- [12] Y. Aharonov and D. Bohm, Phys. Rev. **115**, 485 (1959).
- [13] The plane wave can be considered as the limiting case of a particle in a box and the expansion coefficient $c_n = \lim_{L \rightarrow \infty} \int_{-\frac{L}{2}}^{\frac{L}{2}} \frac{1}{\sqrt{L}} \psi_n(q, t) dq$ ($q = x, y$) vanishes for odd n .
- [14] A. Tomita and R. Chiao, Phys. Rev. Lett. **57**, 937 (1986).
- [15] D. Suter, K. T. Mueller, and A. Pines, Phys. Rev. Lett. **60**, 1218 (1988).
- [16] For more details, see *Geometric Phases in Physics*, edited by A. Shapere and F. Wilczek (World Scientific, Singapore, 1989).

Figure captions

- Fig. 1. The time-dependent potential of a square waveform.
- Fig. 2. The stability-instability diagram. The vertical strips stand for the stable regions in the x -motion, the horizontal strips for the y -motion.
- Fig. 3. The schematic diagram of the experimental arrangement.
- Fig. 4. The shapes of $g_-(t)$ for Table 1. The time is denoted in units of τ .